Int. J. Heat Mass Transfer. Vol. 18, pp. 1343–1350. Pergamon Press 1975. Printed in Great Britain

TRANSIENT FILM BOILING FROM A MOVING SPHERE

K. H. Hsiao,* L. C. Witte† and J. E. Cox‡
University of Houston, Mechanical Engineering Department, Houston, TX 77004, U.S.A.

(*Received* 20 *August* 1974 *and in revised form* 13 *February* 1975)

Abstract—An analytical model is developed to describe the sequence of transient events associated with a hot sphere moving in a cool liquid where a vapor blanket surrounds the sphere. Energy and momentum considerations of each of the coupled regions (the hot sphere, the vapor shell and the surrounding liquid coolant) provide the transient growth of the vapor-film thickness and the heat flux rate from the hot sphere. This phenomenon is closely associated with the interactions of hot molten materials and liquid coolants which may be an important factor in the vapor explosion phenomenon.

NOMENCLATURE

$\bar{A}$, constant, equation (11);
$\bar{B}$, constant, equation (12);
b, constant defined by equation (A16);
c, specific heat;
$\bar{D}$, constant, equation (34);
E, energy;
$\dot{E}$, energy rate;
h_{fg}, latent energy;
k, thermal conductivity;
$\dot{m}$, mass flow rate;
n, integer;
$\bar{N}_1$, dimensionless parameter, equation (A4);
$\bar{N}_2$, dimensionless parameter, equation (A5);
$\bar{N}_3$, dimensionless parameter, equation (A8);
$\bar{N}_4$, dimensionless parameter, equation (A9);
$\bar{N}_5$, dimensionless parameter, equation (A10);
$\bar{N}_6$, dimensionless parameter, equation (38);
P, pressure;
$\overline{Pe}$, Peclet number, equation (14);
Pe, Peclet number, equation (A3);
q'', heat-transfer rate per unit area;
R_1, radius of sphere;
R_2, liquid–vapor interface;
$R(x)$, $R_1 \sin\theta$;
r, radial coordinate;
t, temperature;
U, velocity;
u, tangential velocity component;
v, normal velocity component;
x, curvilinear coordinate;
Y, auxiliary variable, equation (A6);
y, normal coordinate.

Greek symbols

α, thermal diffusivity;
δ, vapor-film thickness;
μ, viscosity;
ρ, density;
τ, time;
$\bar{\tau}$, dimensionless time, equation (13);
τ^*, dimensionless time, equation (A2);
θ, angular coordinate.

Subscripts

0, initial condition;
1, sphere;
2, coolant vapor;
3, liquid coolant;
∞, free stream;
cv, control volume;
w, sphere surface;
sat, saturation.

INTRODUCTION

In recent years, significant progress has been made in understanding the physics of a little-known but highly important phenomenon—explosive vapor formation, or as the overall phenomenon is sometimes called, the vapor explosion. Although there is still some controversy regarding the exact nature and sequence of events that characterize the phenomenon, there is agreement that the initiating event involves intimate contact between hot molten material and liquid coolant. Generally, the hot molten material has a sufficient level of energy such that the initial transient involves a rapid growth of the coolant vapor film adjacent to the molten material region, leading into the establishment of a stable vapor film, during which the hot molten material cools. Eventually, the cooling of the hot region leads to instability of the vapor film and the intimate contact between liquid coolant and hot molten material. In order to predict the point of instability, it is necessary to treat this initial transient. This treatment involves the coupling of all three regions of interest (namely the hot material region, the vapor-film region and the liquid region) to describe adequately the initial heat transfer from the hot material region. The system selected for analysis was motivated from knowledge attained from considerable laboratory experimentation; tests involved the dropping of spherical-shaped (or near spherical-shaped) droplets of various molten metals into liquid coolants. Transient data are also available for the rapid cooling of instrumented solid spheres. The analytical model shown in Fig. 1 includes all three coupled regions: the hot-metal sphere, the coolant vapor film and the surrounding liquid coolant.

*Currently with M. W. Kellogg, Houston, Texas, U.S.A.
†Professor and Chairman.
‡Professor.

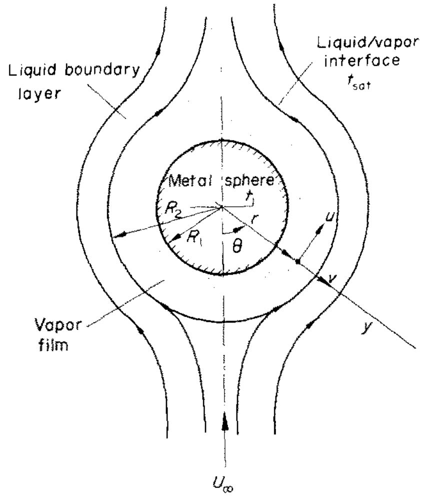

FIG. 1. Metal sphere translating in a coolant undergoing film boiling.

The phenomenon of film boiling around a spherical body with a time-dependent temperature field has not been solved. Existing literature is limited to cases with either the heating-surface temperature or the heat flux maintained constant with time; the heating surfaces are either vertical or horizontal plates or an inclined flat plate. For cases of flat plates, cones and certain other classes of surfaces (bodies of revolution), similarity transformation methods are applicable [1].* The similarity transformation fails for the spherical configuration, thus requiring an approximate method. The phenomenon of transient film boiling must be solved, since this phenomenon represents the initial interaction between the molten material and the coolant. The subsequent events must be based on the results of the transient film-boiling event.

ANALYTICAL MODEL

The complete development of the governing equations (conservation of mass, momentum and energy) for each region along with the appropriate initial, boundary and coupling conditions are presented by Hsiao [2]. However, the basic formulation is provided with supporting discussion and justification or approximations based on experimental observations where appropriate.

Liquid-coolant region

Since vigorous interaction between molten materials and coolants generally occurs only if the coolant is significantly subcooled, an understanding of the overall phenomenon must include the influence of the liquid-coolant region. The film boiling regime as a whole is extremely short. (Say less than one second for many cases of interest.) Thermal and momentum diffusion lengths [$\sqrt{(\alpha\tau)}$ and $\sqrt{(\nu\tau)}$] are correspondingly very short (e.g. in water about 10^{-4} m). The effects of molecular diffusion of both energy and momentum are concentrated in a thin layer near the liquid–vapor interface.

Velocity distribution. The velocity of the liquid around the liquid–vapor interface is assumed to differ insignificantly from potential flow, yielding

$$u_3 = U_\infty\left(1+\frac{R_1^3}{r^3}\right)\sin\theta \tag{1}$$

$$v_3 = -U_\infty\left(1-\frac{R_1^3}{r^3}\right)\cos\theta \tag{2}$$

where $r = R_1+\delta$; and since $\delta \ll R_1$

$$u_3 = \tfrac{3}{2}U_\infty\left(1-\frac{y}{r}\right)\sin\theta \approx \tfrac{3}{2}U_\infty\sin\theta \tag{3}$$

$$v_3 = -3U_\infty\frac{y}{R_1}\cos\theta \tag{4}$$

where y is the distance from the liquid–vapor interface. This assumption is rather common in studies of forced convection film boiling. It simply implies that the drag of the vapor film upon the adjacent liquid is negligibly small.

Stevens in his photographic studies of transient film boiling [6] observed that in highly subcooled water the film is quite thin even past the point on the sphere where a wake usually forms. So, equation (3) is applicable over practically the entire sphere surface.

Temperature distribution. When the hot metal sphere comes into contact with the coolant, a liquid–vapor interface is formed at the saturation temperature. Because of the thin thermal diffusion length, the liquid at a distance outside the thermal layer is at its initial temperature. If the origin of the coordinate system is located at the liquid–vapor interface, then the governing energy equation is

$$\frac{\partial t_3}{\partial\tau}+\frac{u_3}{r}\frac{\partial t_3}{\partial\theta}+v_3\frac{\partial t_3}{\partial r}=\alpha_3\frac{\partial^2 t_3}{\partial r^2} \tag{5}$$

where

$$r = R_1+\delta+y \simeq R_1+y.$$

Substituting equations (3) and (4) into (5) gives

$$\frac{\partial t_3}{\partial\tau}-3U_\infty\cos\theta\frac{y}{R_1}\frac{\partial t_3}{\partial y}+\tfrac{3}{2}U_\infty\sin\theta\frac{1}{R_1}\frac{\partial t_3}{\partial\theta}=\alpha_3\frac{\partial^2 t_3}{\partial y^2}. \tag{6}$$

The liquid coolant is initially at a uniform temperature t_∞ which is below the saturation temperature t_{sat}. At large distances away, the coolant temperature is unaffected. The initial and boundary conditions can be written as

$$t_3(y,\theta,0)=t_\infty \quad \text{when } \tau=0 \tag{7}$$

$$t_3(0,\theta,\tau)=t_{sat} \quad \text{at } y=0 \tag{8}$$

$$t_3(\infty,\theta,\tau)=t_\infty \quad \text{at } y=\infty. \tag{9}$$

The solution of equation (6) for conditions (7)–(9) is given by Chao [3]

$$\bar{t}_3 \equiv \frac{t_3-t_\infty}{t_{sat}-t_\infty}=\frac{1}{1+\bar{A}}\operatorname{erfc}\left\{\frac{\sqrt{(3\bar{Pe})}}{4}\sin^2\theta \times\frac{y}{R_1}\left[\bar{B}-\cos\theta-\tfrac{1}{3}\bar{B}^3+\tfrac{1}{3}\cos^3\theta\right]^{-\frac{1}{2}}\right\} \tag{10}$$

*Numbers in brackets indicate references.

where:

$$\bar{A}^2 \equiv [(k_3\rho_3c_3)/(k_2\rho_2c_2)] \quad (11)$$

$$\bar{B} \equiv \frac{1-\dfrac{1-\cos\theta}{1+\cos\theta}\exp[-\frac{3}{2}(\overline{Pe})\bar{\tau}]}{1+\dfrac{1-\cos\theta}{1+\cos\theta}\exp[-\frac{3}{2}(\overline{Pe})\bar{\tau}]} \quad (12)$$

$$\bar{\tau} \equiv \alpha_3\tau/R_1^2 \quad (13)$$

$$\overline{Pe} \equiv 2U_\infty R_1/\alpha_3. \quad (14)$$

The heat flux at the liquid–vapor interface is

$$q_3'' = -k_3\left[\frac{\partial t_3}{\partial y}\right]_{y=0}$$

$$= \frac{k_3(t_{sat}-t_\infty)}{2R_1}\frac{\sqrt{\dfrac{3}{\pi}\overline{Pe}}}{1+\bar{A}}\sin^2\theta \times[\bar{B}-\cos\theta+\tfrac{1}{3}\cos^3\theta-\tfrac{1}{3}\bar{B}^3]^{-\frac{1}{2}}. \quad (15)$$

Vapor–film region

Velocity distribution. The momentum equation for the vapor film flowing around a sphere can be written as

$$\rho_2\left(\frac{\partial u_2}{\partial\tau}+u_2\frac{\partial u_2}{\partial x}+v_2\frac{\partial u_2}{\partial y}\right) = -\frac{\partial P}{\partial x}+\mu_2\frac{\partial^2u_2}{\partial y^2}. \quad (16)$$

A curvilinear x–y coordinate system is used in equation (16) with x coinciding with the sphere surface and y being normal to the surface. In free convective cases the pressure gradient term would represent the hydrostatic pressure head. However, in this case, where flow effects are dominant over bouyancy and hydrostatic head, the pressure gradient along the sphere surface will be related to the velocity field in the liquid around the sphere, as will be shown later. At the surface of the sphere,

$$u_2(x,0,\tau) = v_2(x,0,\tau) = 0 \quad (17)$$

and at the liquid–vapor interface

$$u_2(x,\delta,\tau) = u_3 = \tfrac{3}{2}U_\infty\sin\theta. \quad (18)$$

Following the results of Witte [4], inertia effects in the vapor film can be neglected so that the momentum relation reduces to

$$\frac{\partial P}{\partial x} = \mu_2\frac{\partial^2u_2}{\partial y^2}. \quad (19)$$

Equation (19) can be integrated twice with respect to y to provide the velocity distribution in the vapor film.

$$u_2(x,y,\tau) = \tfrac{3}{2}U_\infty\sin\theta\frac{y}{\delta}+\frac{1}{2\mu_2}\frac{\partial P}{\partial x}(y^2-y\delta). \quad (20)$$

The variation in pressure in the x-direction can be evaluated from Bernoulli's equation (neglecting elevation effects)

$$P_0 = P+\tfrac{1}{2}\rho_2u_2^2 = \text{constant} \quad (21)$$

so that

$$\frac{\partial P}{\partial x}+\rho_2u_2\frac{\partial u_2}{\partial x} = 0. \quad (22)$$

Using u_2 at the liquid–vapor interface as given by equation (18), the pressure gradient described by equation (22) becomes

$$\frac{\partial P}{\partial x} = -\tfrac{9}{4}\frac{\rho_2U_\infty^2}{R_1}\cos\theta\sin\theta. \quad (23)$$

Substitution of equation (23) into equation (20) will yield the vapor velocity distribution in terms of both angular and y-direction dependence.

Temperature distribution. For the case of film boiling, the temperature and velocity boundary-layer thicknesses coincide. If the convection terms are neglected in the energy equation, the temperature distribution in the vapor film is

$$\frac{t_2(y,\theta,\tau)-t_{sat}}{t_w-t_{sat}} = 1-\frac{y}{\delta} \quad (24)$$

where δ varies with time and angular location and t_w is the interface temperature between the sphere and the vapor.

Metal–sphere region

Any circulation in a hot molten material is relatively small and internal momentum consideration need not be included.

Temperature distribution. The energy equation for the cooling sphere with conduction only in the radial direction is

$$\frac{\partial^2t_1}{\partial r^2}+\frac{2}{r}\frac{\partial t_1}{\partial r} = \frac{1}{\alpha_1}\frac{\partial t_1}{\partial\tau} \quad (25)$$

where the sphere is initially at a uniform temperature t_{01} which is above the saturation temperature t_{sat} of the surrounding coolant

$$t_1(r,0) = t_{01} \quad (26)$$

The solution of equation (25) is

$$\frac{t_1(r,\tau)-t_{01}}{t_w-t_{01}} = \frac{R_1}{r}\sum_{n=0}^{\infty}\left\{\text{erfc}\left[\frac{(2n+1)R_1-r}{2\sqrt{(\alpha_1\tau)}}\right] - \text{erfc}\left[\frac{(2n+1)R_1+r}{2\sqrt{(\alpha_1\tau)}}\right]\right\}. \quad (27)$$

Using this temperature distribution in the Fourier's relation, the heat flux from the sphere becomes

$$q_1'' = \frac{k_1}{R_1}(t_{01}-t_w) \times\left[\frac{R_1}{\sqrt{(\pi\alpha_1\tau)}}\left(1+2\sum_{n=0}^{\infty}\exp\left(\frac{-n^2R_1^2}{\alpha_1\tau}\right)\right)-1\right] \quad (28)$$

Vapor-film thickness

The difference between the energy transferred from the sphere to the vapor film q_1'' and the energy transferred from the vapor film to the surrounding liquid q_3'' represents the rate of change of the energy level of the vapor film. The net energy flow to or from the vapor region can involve a change in the sensible energy of the vapor film and the latent energy associated with evaporation (or condensation) of coolant at the liquid–

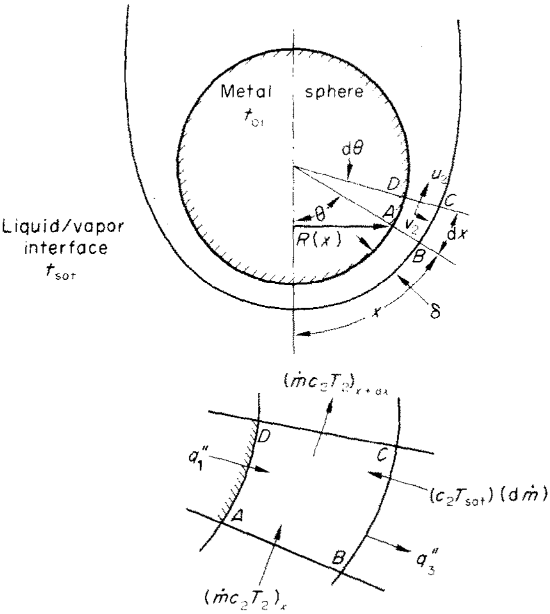

FIG. 2. Energy balance for a control volume in the vapor film.

vapor interface. If an elemental volume of the vapor film is selected as shown in Fig. 2, an energy balance can be written which can be used to relate the vapor film thickness to both position and time. The change in the mass flow rate of vapor between x and $x+dx$ is

$$d\dot{m} = \frac{\partial}{\partial x}\left[R(x)\int_0^\delta \rho_2 u_2\,dy\right]dx. \quad (29)$$

The energy rate into the control volume can be expressed as

$$\dot{E}_{in} = R(x)q_1''\,dx + R(x)\int_0^\delta \rho_2 u_2 c_2 t_2\,dy + c_2 t_{sat}\,d\dot{m} \quad (30)$$

and the energy rate out of the control volume is

$$\dot{E}_{out} = R(x)q_3''\,dx + R(x)\int_0^\delta \rho_2 u_2 c_2 t_2\,dy + \frac{\partial}{\partial x}\left[R(x)\int_0^\delta \rho_2 u_2 c_2 t_2\,dy\right]dx + h_{fg}'\,d\dot{m} \quad (31)$$

the rate of energy change in the control volume is given as

$$\left(\frac{\partial E}{\partial \tau}\right)_{c.v.} = \frac{\partial}{\partial \tau}\left[R(x)\int_0^\delta \rho_2 c_2 (t_2 - t_{sat})\,dy\right]dx. \quad (32)$$

Equations (30)–(32) can be combined to provide the energy-expression for the vapor film. Equation (24) provides the variation of t_2 and equation (20) involves the application of thin film concept ($\delta \ll R_1$), i.e. equation (3). Calculations show that the film gets relatively thick between 170 and 180 degrees on the sphere surface. This has very little effect, however, on the total heat flux from the sphere, since only a small fraction of the total area is involved. Rigorously, however, the solution is limited to angles less than about 170 degrees. Equation (29) can be substituted for q_1'' and equation (15) can be substituted for q_3''.

Equation (24) expresses t_2 in dimensionless form involving the interface temperature between the sphere and vapor, t_w; this interface temperature can be estimated by the relation

$$t_w - t_{sat} = \frac{t_{01} - t_{sat}}{\bar{D}}, \quad (33)$$

where

$$\bar{D} \equiv 1 + \frac{k_2}{k_1}\sqrt{\left(\frac{\alpha_1}{\alpha_2}\right)}. \quad (34)$$

This estimation of the interface temperature [4] is based on conduction when two bodies with initial temperatures of t_{01} and t_{sat} come into contact. The interface temperature is independent of time. If the energy integral equation is integrated with respect to y, the resulting differential equation for the vapor-film thickness is

$$\frac{\partial \delta}{\partial \tau} + \frac{U_\infty}{2R(x)}\left\{1 + \frac{3h_{fg}\bar{D}}{c_2(t_{01} - t_{sat})}\right\}\frac{\partial}{\partial x}[\delta R(x)\sin\theta] = \frac{2\sqrt{(\alpha_1\alpha_2)}}{R_1}\left[\frac{R_1}{\sqrt{(\pi\alpha_1\tau)}} - 1\right] - \frac{k_3\bar{D}}{R_1\rho_2 c_2} \times \frac{(\bar{B} - \cos\theta - \frac{1}{3}\bar{B}^3 + \frac{1}{3}\cos^3\theta)^{-\frac{1}{3}}}{1+\bar{A}} \times \left(\frac{t_{sat} - t_\infty}{t_{01} - t_{sat}}\right)\sqrt{\left(\frac{6U_\infty R_1}{\pi\alpha_3}\right)}\sin^2\theta \quad (35)$$

the solution of equation (35) provides the transient response of the vapor-film thickness. The solution is outlined in the Appendix.

The heat flux from the surface of the sphere can be estimated from equation (28) expressed in terms of t_{sat} rather than t_w as

$$q_1'' = \frac{k_1(t_{01} - t_{sat})}{R_1}\frac{\bar{D} - 1}{\bar{D}}\left[\sqrt{\left(\frac{R_1^2}{\pi\alpha_1\tau}\right)} - 1\right] \quad (36)$$

which can be approximated by

$$\frac{q_1'' R_1}{k_1(t_{01} - t_{sat})} = \bar{N}_6\left[\frac{1}{\bar{N}_3}\sqrt{\left(\frac{4R_1}{\pi\alpha_1\tau}\right)} - 1\right] \quad (37)$$

where

$$\bar{N}_6 \equiv \bar{D} - 1. \quad (38)$$

NUMERICAL RESULTS

Because all three regions (liquid, vapor, and sphere) are coupled in the solution, there are many factors influencing the transient growth of the vapor film. The possible combinations of factors, which could have an influence on the results, are too numerous to include in a realistic manner. For example, the thermal diffusivities of all three regions could be important in the development of the vapor film. Fortunately, the thermal diffusivities of the vapor and the liquid coolant are uniquely related, i.e. the vapor and liquid are different phases of the same substance and hence dependent upon the temperatures and pressures involved; one is not completely independent of the other.

The numerical results are presented in terms of dimensionless parameters which arise naturally in the development of the governing equations as shown in the Appendix. In some instances, the physical meaning of the parameters is obvious (e.g. $\bar{N}_3$ represents relative importance of the sphere and vapor region diffusivities on the transient growth). Other parameters, however, are more complex and any physical meaning is complicated. The objective of the calculation is to investigate the influence of these parameters on the vapor growth around a spherical region. Actually, $\bar{N}_3$ through $\bar{N}_6$ are used in the parametric study but the influence of $\bar{N}_1$ and $\bar{N}_2$ is included along with the additional influence of velocity represented by the Peclet number. When possible, comparison to experimental observations are made to show the applicability of the model to the actual case. There is, however, rather a dearth of directly comparable experimental data for this particular phenomenon. The parameters' ranges are selected to encompass the experimental conditions for several investigations involving the dropping of molten aluminum, bismuth, tin, mercury, lead, and zinc into water, liquid sodium and liquid nitrogen; several hydrocarbons (CH_4, C_3H_8 and C_2H_6) contacting water could conceivably be included in the parameter ranges.

Figures 3 and 4 show the angular dependence of the vapor film calculated at specific time intervals. In both cases, it is apparent that in the initial growth stages ($\bar{\tau} < 10^{-5}$) the growth is dominated by purely conductive effects (i.e. the thickness is not dependent upon angle). However, as the film develops, the vapor film becomes tear-drop shaped surrounding the sphere, indicative of the influence of convective effects. This shape is in agreement with experimental observations [6].

The Peclet number is 1400 for both Figs. 3 and 4, so no velocity effect is represented by a comparison between the two figures. However, the parameters $\bar{N}_3$, $\bar{N}_4$ and $\bar{N}_5$ are varied between the two plots. Figure 3 represents a case where the thermal diffusivity of the sphere material is the same as the vapor while Fig. 4 represents the case where sphere thermal diffusivity is considerably higher than that of the vapor region; the effect is a dramatic decrease in the time required for the development of the film. The effect of increasing $\bar{N}_5$ for this particular situation can be interpreted physically to represent an increase in subcooling of the surrounding liquid. This effect also tends to cause the film to develop faster and to be thinner at any time after the initiation of the growth. A comparison of Figs. 3 and 4 show that this trend is indeed the case.

Further investigation of these effects are shown in Figs. 5 and 6. Figure 5 clearly demonstrates that increasing the liquid subcooling causes a thinner liquid film (especially over the forward portion of the spherical region). The effect of diffusivity in Fig. 6 suggests that perhaps the subcooling of the liquid has a stronger effect upon the thickness of the film. It should be noted, however, that Fig. 6 describes a time at which convective effects are beginning to dominate in the vapor and liquid regions.

Figure 7 demonstrates the effect of the variation of the parameter $[h_{fg}/c_2(t_{01}-t_{sat})]$ which is contained in $\bar{N}_4$; this represents the effect of changing the sphere initial temperature for a given liquid coolant pressure; or conversely, it would also represent the effect of a pressure change on h_{fg}. For either case, the results are consistent with physical reasoning; if the temperature difference across the film is increased, $\bar{N}_4$ decreases, and the conductive effects are high (yielding a thicker film especially over the forward portion of the sphere). Likewise, an increase in h_{fg} indicates that more energy is required to form the vapor; the vapor is thinner and no doubt convective effects dominate more quickly. Figure 7 verifies this situation.

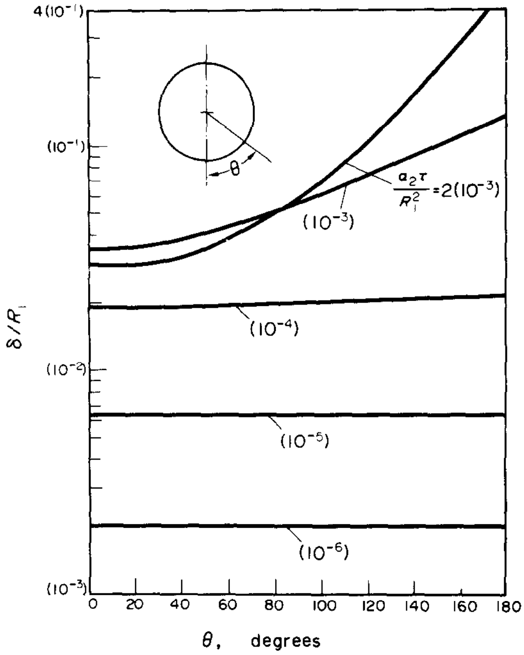

FIG. 3. Transient vapor-film thickness variation for $\bar{N}_3 = 1$, $\bar{N}_4 = 500$, $\bar{N}_5 = 0{\cdot}5$ and $Pe = 1400$.

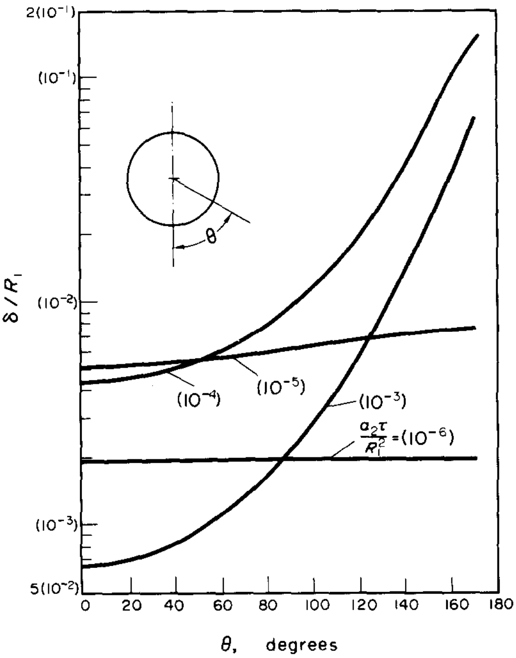

FIG. 4. Transient vapor-film thickness variation for $\bar{N}_3 = 4$, $\bar{N}_4 = 15\,000$, $\bar{N}_5 = 1{\cdot}5$ and $Pe = 1400$.

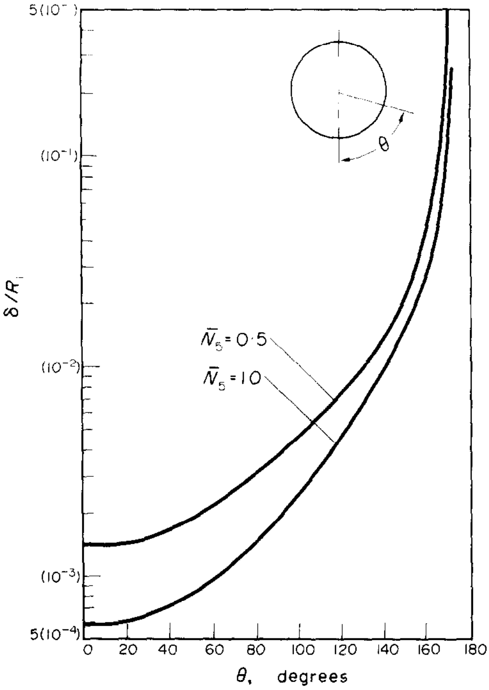

FIG. 5. Dependence of vapor-film thickness on the $\bar{N}_5$ parameter for $\bar{N}_3 = 4$, $\bar{N}_4 = 10\,000$, $Pe = 1400$ and $\alpha_2 \tau / R_1^2 = 4{\cdot}5(10^{-4})$.

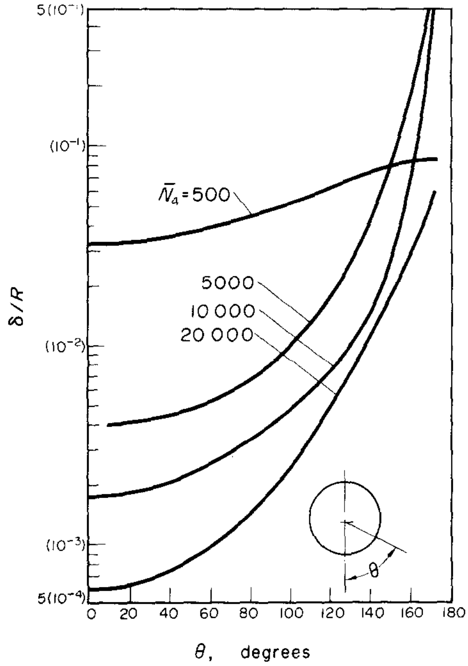

FIG. 7. Dependence of vapor-film thickness on the $\bar{N}_4$ parameter for $\bar{N}_3 = 4$, $\bar{N}_5 = 1{\cdot}5$, $Pe = 1400$ and $\alpha_2 \tau / R_1^2 = 7{\cdot}5(10^{-4})$.

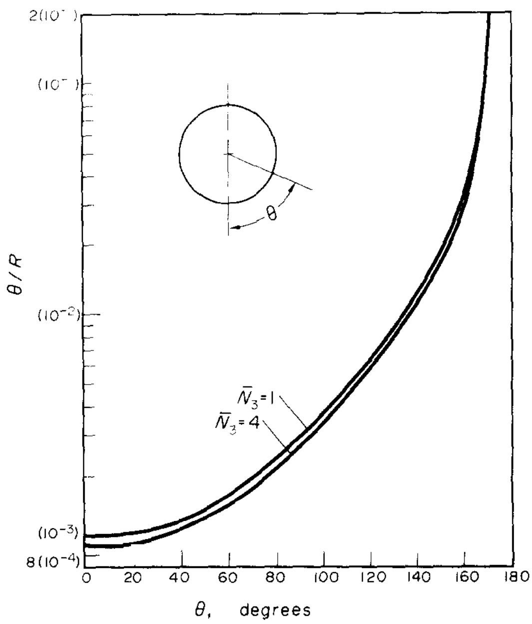

FIG. 6. Dependence of vapor-film thickness on the $\bar{N}_3$ parameter for $\bar{N}_4 = 15\,000$, $\bar{N} = 1{\cdot}5$, $Pe = 1400$ and $\alpha_2 \tau / R_1^2 = 7{\cdot}5(10^{-4})$.

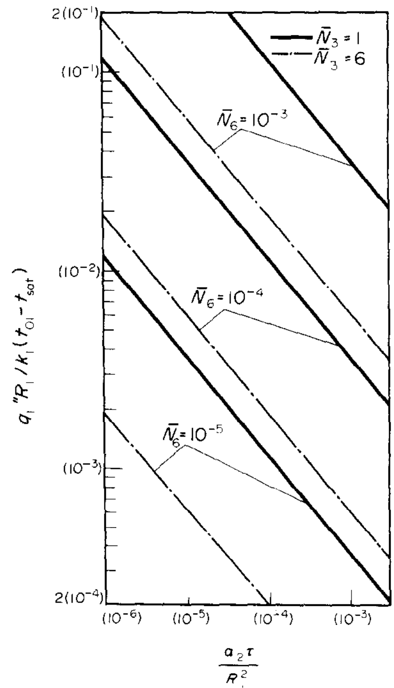

FIG. 8. Heat flux at the metal sphere surface for $\bar{N}_3 = 1$ and $\bar{N}_3 = 6$ for $\bar{N}_6 = 10^{-3}$, 10^{-4} and 10^{-5}.

The heat flux from the sphere surface is given by equation (37) and is a function of only $\bar{N}_3$ and $\bar{N}_6$ (i.e. the heat flux is controlled by the thermal properties of the vapor and spherical region during the rapid-growth phase. Figure 8 illustrates the variation of heat flux for wide ranges of $\bar{N}_1$ and $\bar{N}_6$. The heat flux rapidly decays with time. This, in conjunction with the increasing dominance of convection as time proceeds, accounts for the growth and then the decrease in thickness of the vapor film.

SUMMARY

The transient growth of vapor adjacent to a surface (which is above the temperature at which film boiling occurs) has been modeled, including the coupling of all three regions of importance. Equation (35), which describes the transient growth of the vapor, reverts (in the limit for long times) to the formulation for steady-state boiling from a uniform wall temperature spherical region.

Solutions to the equations (for a range of parameters limited to values typical of prior experiments) show consistency with physical reasoning and experimental observations. Stevens [6] for example, estimated the vapor-film thicknesses around 2·54-cm dia silver sphere during transient boiling. He found that the thicknesses were on the order of $2{\cdot}5 \times 10^{-2}$ cm. Calculations by the model for a 2-cm sphere and for the same conditions as Stevens' data yield a range of film thicknesses from 10^{-3} cm at the stagnation point to about 10^{-2} cm over the rear portion of the sphere. The average of these two values is very close to Steven's estimate. The importance of liquid subcooling is very apparent from the calculations. Subcooling causes a quicker development of the vapor region into a stable, thinner film over the front portion of the sphere.

Acknowledgement—The authors express their gratitude to the USAEC for support of this work under contract AT-(40-1)-3936.

REFERENCES

1. J. F. Harper, The motion of bubbles and drops through liquids, *Adv. Appl. Mech.* Vol. 12, pp. 59–124. Academic Press, New York (1973).
2. K.-H. Hsiao, Molten metal/water interactions prior to a vapor explosion, Ph.D. Dissertation, University of Houston (May 1974).
3. B. T. Chao, Transient heat and mass transfer to a translating droplet, *J. Heat Transfer* **91**(2), 273–281 (May 1969).
4. L. C. Witte, Heat transfer from a sphere to liquid sodium during forced convection, Argonne National Laboratory, ANL-7296 (1967).
5. J. W. Stevens, L. C. Witte and J. E. Cox, The vapor explosion—heat transfer and fragmentation—VI. Transition film and transition boiling from a sphere, University of Houston Report No. ORO-3936-9 (September 1972).
6. J. W. Stevens and L. C. Witte, Transient film and transition boiling from a sphere, *Int. J. Heat Mass Transfer* **14**, 443–450 (1971).
7. E. Ruckenstein and E. J. Davis, The effects of bubble translation on vapor bubble growth in a superheated liquid, *Int. J. Heat Mass Transfer* **14**, 939–952 (1971).

APPENDIX A

Equation (35) can be written in terms of dimensionless parameters as

$$\frac{\partial(\delta/R_1)}{\partial\tau^*}+\frac{\bar{N}_1 Pe}{\sin\theta}\frac{\partial}{\partial\theta}\left(\frac{\delta}{R_1}\sin^2\theta\right) = \frac{2}{\sqrt{(\pi\tau^*)}}-2\left(\frac{\alpha_1}{\alpha_2}\right)^{\frac{1}{2}}-\bar{N}_2(Pe)^{\frac{1}{2}}\bar{B}\sin^2\theta \quad \text{(A1)}$$

where

$$\tau^* \equiv \alpha_2\tau/R_1^2 \quad \text{(A2)}$$

$$Pe \equiv R_1 U_\infty/\alpha_2 \quad \text{(A3)}$$

$$\bar{N}_1 \equiv \frac{1}{2}\left[1+\frac{3\bar{D}h_{fg}}{c_2(t_{01}-t_{\text{sat}})}\right] \quad \text{(A4)}$$

$$\bar{N}_2 \equiv \frac{\bar{D}\sqrt{\left(\frac{6}{\pi}\right)}}{1+\bar{A}}\,\frac{k_3}{k_2}\left(\frac{\alpha_2}{\alpha_3}\right)^{\frac{1}{2}}\left(\frac{t_{\text{sat}}-t_\infty}{t_{01}-t_{\text{sat}}}\right). \quad \text{(A5)}$$

If an auxiliary variable $Y(\theta, \tau^*)$ is introduced

$$Y(\theta,\tau^*) \equiv \sin^2\theta\left[\frac{\delta(\theta,\tau^*)}{R_1}\right] \quad \text{(A6)}$$

and employed in equation (A1), the expression for the vapor-film thickness becomes

$$\frac{\partial Y}{\partial\tau^*}+\bar{N}_4\sin\theta\frac{\partial Y}{\partial\theta} = -\bar{N}_3\sin^2\theta+\frac{2}{\sqrt{\pi}}\sin^2\theta\frac{1}{\sqrt{(\tau^*)}} -\bar{N}_5[\bar{B}-\cos\theta-\tfrac{1}{3}\bar{B}^3+\tfrac{1}{3}\cos^3\theta]^{-\frac{1}{2}}\sin^4\theta. \quad \text{(A7)}$$

where

$$\bar{N}_3 \equiv 2\sqrt{\left(\frac{\alpha_1}{\alpha_2}\right)} \quad \text{(A8)}$$

$$\bar{N}_4 \equiv \bar{N}_1 Pe \quad \text{(A9)}$$

$$\bar{N}_5 \equiv \bar{N}_2\sqrt{(Pe)}. \quad \text{(A10)}$$

The auxiliary variable $Y(\theta, \tau^*)$ must be an even function with respect to the angular coordinate, i.e. $Y(\theta, \tau^*) = Y(-\theta, \tau^*)$. The first-order partial differential equation (A7) is solved by equation by the method of characteristics. Equation (A7) can be transformed into the corresponding characteristic system

$$\frac{d(\tau^*)}{1}=\frac{d\theta}{\bar{N}_4\sin\theta}=\frac{dY}{-\bar{N}_3\sin^2\theta+\frac{2\sin^2\theta}{\sqrt{(\pi\tau^*)}}-\bar{N}_5\sin^4\theta[\bar{B}-\cos\theta-\frac{1}{3}\bar{B}^3+\frac{1}{3}\cos^3\theta]^{-\frac{1}{2}}} \quad \text{(A11)}$$

which can result into two equations. The first equation to be solved is

$$\frac{d(\tau^*)}{1}=\frac{d\theta}{\bar{N}_4\sin\theta} \quad \text{(A12)}$$

which has the solution

$$\ln\left(\tan\frac{\theta}{2}\right)=\bar{a}+\bar{N}_4\tau^* \quad \text{(A13)}$$

where $\bar{a}$ is an integration constant. The second equation is

$$\frac{d(\tau^*)}{1}=\frac{dY}{-\bar{N}_3\sin^2\theta+\frac{2\sin^2\theta}{\sqrt{(\pi\tau^*)}}-\bar{N}_5\sin^4\theta[\bar{B}-\cos\theta-\frac{1}{3}\bar{B}^3-\frac{1}{3}\cos^3\theta]^{-\frac{1}{2}}} \quad \text{(A14)}$$

Using trigonometric relations involving $\theta/2$ and equation (A13), equation (A14) becomes

$$\frac{\mathrm{d}Y}{\mathrm{d}(\tau^*)} = \frac{-4\bar{N}_3 \exp[2\bar{a}+\bar{N}_4\tau^*]}{1+\exp[2\bar{a}+\bar{N}_4\tau^*]} + \frac{8\exp[2(\bar{a}+\bar{N}_4\tau^*)]}{\sqrt{(\pi\tau^*)}[1+\exp[2(\bar{a}+\bar{N}_4\tau^*)]]^2} \times \frac{-16\bar{N}_5 \exp[4(\bar{a}+\bar{N}_4\tau^*)]}{[1+\exp\{2(\bar{a}+\bar{N}_4\tau^*)\}]^4} \left\{ \frac{1-\exp[-3Pe+2\bar{a}+2\bar{N}_4\tau^*]}{1+\exp[-3Pe+2\bar{a}+2\bar{N}_4\tau^*]} - \frac{1-\exp[2(\bar{a}+\bar{N}_4\tau^*)]}{1+\exp[2(\bar{a}+\bar{N}_4\tau^*)]} + \frac{1}{3}\frac{1-\exp[2(\bar{a}+\bar{N}_4\tau^*)]}{1+\exp[2(\bar{a}+\bar{N}_4\tau^*)]} - \frac{1}{3}\left[\frac{1-\exp[-3+2\bar{a}+2\bar{N}_4\tau^*]}{1+\exp[-3+2\bar{a}+2\bar{N}_4\tau^*]}\right]^3 \right\}^{-\frac{1}{2}} \tag{A15}$$

Equation (A15) can be integrated with respect to dimensionless time yielding another constant of integration b. The general solution of equation (A7) is of the form

$$b = F(\bar{a}) = F\left(-\bar{N}_4\tau^* + \ln\left[\tan\frac{\theta}{2}\right]\right). \tag{A16}$$

The initial condition is based on the vapor-film growth beginning with $\tau = 0$

$$\delta(\theta, 0) = 0. \tag{A17}$$

If equation (A15) is integrated, if the integration constant $\bar{b}$ is substituted from equation (A16) and if the initial condition equation (A17) is employed, the vapor-film thickness is obtained. The integration is performed numerically by the 4-point, Gauss–Legendre quadrature.

EBULLITION EN FILM TRANSITOIRE SUR UNE SPHERE EN MOUVEMENT

Résumé—Un modèle analytique est développé afin de décrire la suite des phénomènes transitoires qui accompagnent le mouvement d'une sphère chaude dans un liquide froid lorsqu'un matelas de vapeur entoure la sphère. Des considérations énergétiques et dynamiques relatives à chacune des régions couplées (la sphère chaude, l'enveloppe de vapeur et de liquide froid environnant) précisent l'augmentation transitoire de l'épaisseur du film de vapeur et de flux thermique sur la sphère chaude. Ce phénomène est étroitement lié aux intéractions entre des matériaux fondus chauds et des liquides de refroidissement qui peuvent représenter un facteur important dans le phénomène de vaporisation explosive.

INSTATIONÄRES FILMSIEDEN AN EINER BEWEGTEN KUGEL

Zusammenfassung—Es wird ein analytisches Modell aufgestellt zur Beschreibung der aufeinanderfolgenden instationären Ereignisse, wenn sich durch eine kalte Flüssigkeit eine heiße, von einem Dampffilm umgebene Kugel bewegt. Energie- und Impulsbetrachtungen für jeden der gekoppelten Bereiche (die heiße Kugel, der Dampffilm und das äußere flüssige Kühlmittel) führen zu Ausdrücken für das instationäre Wachstum des Dampffilms und für den Wärmestrom von der heißen Kugel. Dieses Phänomen ist eng mit den Wechselwirkungen zwischen heißen, geschmolzenen Materialien und flüssigen Kühlmitteln verknüpft und könnte einen wichtigen Faktor bei Dampfexplosionsphänomenen darstellen.

НЕСТАЦИОНАРНОЕ ПЛЕНОЧНОЕ КИПЕНИЕ НА ПЕРЕМЕЩАЮЩЕЙСЯ СФЕРЕ

Аннотация — Разработана аналитическая модель для описания ряда нестационарных процессов, последовательно протекающих при перемещении горячей сферы в холодной жидкости с образованием вокруг сферы паровой оболочки. Учет энергии и количества движения для каждой из взаимодействующих областей (горячая сфера, паровая оболочка и окружающая холодная жидкость) позволил определить рост толщины паровой пленки и изменение интенсивности теплового потока от горячей сферы. Это явление близко к взаимодействию горячих расплавов с жидкими охладителями и может служить важным фактором в возникновении явления парового взрыва.